PHYSICAL REVIEW B **87**, 241404(R) (2013)

Engineering quantum spin Hall effect in graphene nanoribbons via edge functionalization

Gabriel Autès and Oleg V. Yazyev
Institute of Theoretical Physics, Ecole Polytechnique Fédérale de Lausanne (EPFL), CH-1015 Lausanne, Switzerland
(Received 22 November 2012; published 17 June 2013)

Kane and Mele predicted that in the presence of spin-orbit interaction graphene realizes the quantum spin Hall state [Phys. Rev. Lett. **95**, 226801 (2005)]. However, exceptionally weak intrinsic spin-orbit splitting in graphene ($\approx 10^{-5}$ eV) inhibits experimental observation of this topological insulating phase. To circumvent this problem, we propose an approach towards controlling spin-orbit interactions in graphene by means of covalent functionalization of graphene edges with functional groups containing heavy elements. Proof-of-concept first-principles calculations show that very strong spin-orbit coupling can be induced in realistic models of narrow graphene nanoribbons with tellurium-terminated edges. We demonstrate that electronic bands with strong Rashba splitting as well as the quantum spin Hall state spanning broad energy ranges can be realized in such systems. Our work thus helps pave the way towards engineering topological electronic phases in nanostructures based on graphene and other materials by means of locally introduced spin-orbit interactions.

DOI: 10.1103/PhysRevB.87.241404 PACS number(s): 73.43.−f, 72.25.Dc, 73.22.Pr, 81.05.ue

In their pioneering paper, Kane and Mele showed that, in the presence of spin-orbit coupling, graphene becomes a two-dimensional Z_2 topological insulator or, in other words, realizes the quantum spin Hall (QSH) state.[1] This topologically nontrivial insulating phase is characterized by the presence of spin-filtered edge states protected from elastic backscattering and localization by time-reversal symmetry. While the prediction of Kane and Mele contributed tremendously to the development of the emerging field of topological insulators,[2–4] the QSH effect in graphene still needs to be observed experimentally, the reason being that the exceptionally weak intrinsic spin-orbit coupling in graphene results in a band gap of the order of only 10^{-5} eV, according to recent theoretical predictions.[5–7]

Subsequent efforts have focused on circumventing the problem of weak intrinsic spin-orbit coupling in graphene. One proposed approach for enhancing spin-orbit interactions is based on the effect of adatoms on the electronic structure of graphene.[8,9] More recently, several groups have demonstrated theoretically that, by depositing the adatoms of heavy elements with large magnitudes of atomic spin-orbit splitting, it is possible to increase the spin-orbit gap up to tens of meV.[10–13] However, realizing such a strategy in practice will inevitably face the challenge of uniform deposition since adatoms are mobile[14,15] and tend to form aggregates due to attractive interactions. Moreover, large metal adatom coverages that are required for enhancing spin-orbit coupling in graphene result in strong doping[11,14,15] while covalently bonded species such as hydrogen adatoms give rise to undesired resonant states.[16,17]

In this Rapid Communication, we propose an alternative approach for engineering spin-orbit interactions in graphene based on covalent chemical functionalization of the edges. The edges of graphene nanostructures provide a natural interface for coupling heavy-element functional groups to the π-electron states of graphene. By using a modification of the Kane-Mele model we show that, by introducing the spin-orbit interaction locally, only at the edges, it is possible to realize the QSH state in narrow graphene nanoribbons. We then focus our attention on realistic models of tellurium- (Te-) terminated graphene nanoribbons which can be produced using current methods of synthetic chemistry. Our first-principles calculations show that very strong spin-orbit coupling can be induced in narrow Te-terminated graphene nanoribbons. In particular, we discuss in detail two configurations that exhibit the presence of a parabolic band with strong Rashba splitting and a robust QSH state spanning a broad energy range, respectively.

The band structure of graphene nanoribbons can be described accurately by using the one-orbital nearest-neighbor tight-binding model. Following Kane and Mele, it is possible to include the intrinsic spin-orbit coupling by adding a second-nearest-neighbor complex term with the sign dependent on the spin of the electron and the hopping direction.[1] The resulting Hamiltonian reads

$$\mathcal{H} = -t \sum_{\langle i,j\rangle,\sigma} c^{\dagger}_{i\sigma} c_{j\sigma} + i\lambda_{\mathrm{so}} \sum_{\langle\langle i,j\rangle\rangle,\sigma} \nu_{ij} c^{\dagger}_{i\sigma} \sigma_z c_{j\sigma}, \qquad (1)$$

where $\langle i,j\rangle$ and $\langle\langle i,j\rangle\rangle$ indicate the pairs of first and second nearest neighbors [Fig. 1(a)], respectively, and σ is the spin index. The parameter $t \approx 2.7$ eV is the tight-binding hopping energy[18] while λ_{so} defines the strength of spin-orbit coupling. $\nu_{ij} = \pm 1$ is the site-dependent Haldane factor given by $\nu_{ij} = (\mathbf{d}_{ik} \times \mathbf{d}_{jk})/|\mathbf{d}_{ik} \times \mathbf{d}_{jk}|$, with $\mathbf{d}_{ik}$ and $\mathbf{d}_{jk}$ being the vectors connecting second nearest neighbors i and j with their common neighbor k.[19] σ_z is the corresponding Pauli matrix describing the spin of the electron.

The introduction of the spin-orbit term opens a band gap $\Delta_{\mathrm{so}} = 6\sqrt{3}\lambda_{\mathrm{so}}$ at the Dirac points of otherwise semimetallic graphene, making it a two-dimensional Z_2 topological insulator. When one-dimensional nanostructures of graphene are considered, spin-orbit coupling lifts the degeneracy of zero-energy edge states,[20–22] resulting in a crossing of linear dispersion bands, as illustrated in Fig. 1(b) for the case of a narrow graphene strip (nanoribbon). At this band crossing the electronic states of opposite spins are localized at the opposite edges of the nanoribbon while time-reversal symmetry is preserved. In other words, the nanoribbon is in the QSH state.

Let us now consider a situation in which spin-orbit interactions are introduced only at the edges due to, for instance, the presence of heavy-element functional groups terminating the edge. One can expect that such local spin-orbit coupling

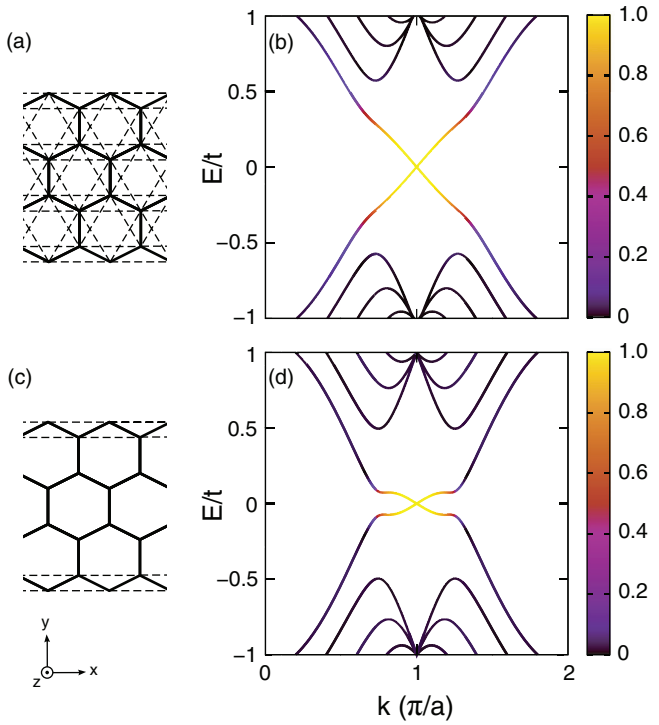

FIG. 1. (Color online) (a) Lattice model and (b) band structure of a narrow zigzag graphene nanoribbon within the Kane-Mele model at $\lambda_{so} = 0.1t$. Solid lines in the lattice model correspond to the nearest-neighbor hoppings while dashed lines indicate all possible pairs of second-nearest-neighbor hoppings summed in the second term of Hamiltonian (1). (c) In the modified Kane-Mele model only second-nearest-neighbor hoppings involving edge atoms are taken into account, resulting in the band structure shown in (d). The bands are colored according to the magnitude of QSH marker $\mathcal{M}_{ik}$.

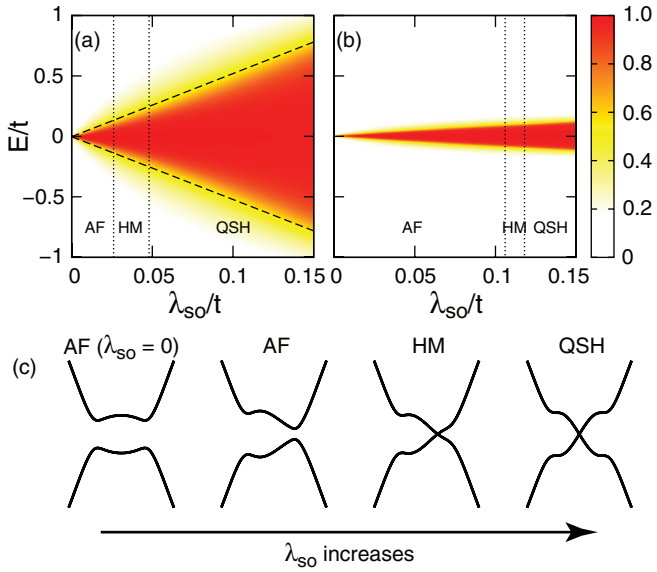

FIG. 2. (Color online) Magnitude of the QSH marker $\mathcal{M}_{ik}$ as a function of energy E and spin-orbit coupling strength λ_{so} for a zigzag nanoribbon in the Kane-Mele model with (a) a full spin-orbit coupling term and (b) spin-orbit interactions introduced only at the edges. The dashed lines in (a) indicate the bulk spin-orbit gap Δ_{so}. The dotted lines delimit the regions of existence of electronic phases driven by electron-electron interactions. (c) Schematic drawing of the evolution of edge-state band dispersion upon increasing λ_{so} in the presence of electron-electron interactions.

will have a significant effect on the π-electron states in graphene due to finite size effects and the fact that low-energy states in graphene nanostructures are strongly localized at the edges.[20,23] In order to model this situation, we restrict summation in the second term of Hamiltonian (1) only to the pairs of second-nearest-neighbor atoms located at the edge, as shown in Fig. 1(c). As in the case of the standard Kane-Mele model, the resulting band structure calculated using the same magnitude of $\lambda_{so} = 0.1t$ exhibits a band crossing at $k = \pi/a$ [Fig. 1(d)].

In order to identify the presence of the QSH state, we propose a simple marker function which signalizes the spin-filtered character of electronic states. For state i of momentum k, we calculate the vectorial quantity with components

$$\mathcal{M}_{ik}^{\alpha} = \frac{2}{W} \int \psi_{ik}^{\dagger}(\mathbf{r}) y \sigma_{\alpha} \psi_{ik}(\mathbf{r}) d\mathbf{r}, \qquad (2)$$

where W is the width of the nanoribbon and σ_{α} are the Pauli matrices ($\alpha = x,y,z$). By convention, we assume that the y direction is transverse to the nanoribbon and lies in its plane; $y = 0$ is located in the middle of the nanoribbon. Ordinary spin-degenerate states are characterized by $|\mathcal{M}_{ik}| = 0$ while the maximum magnitude $|\mathcal{M}_{ik}| = 1$ corresponds to spin-filtered states that are completely localized on the edge atoms. In the presence of time-reversal symmetry, a nonzero magnitude of $\mathcal{M}_{ik}$ indicates the QSH phase while its direction corresponds to the spin direction of the edge state. In the case of the Kane-Mele model with all second-nearest-neighbor atoms summed, the edge states are fully spin filtered in a broad energy range [Fig. 1(b)]. Importantly, the model with spin-orbit interactions introduced at the edges only also results in complete spin filtering, but the energy range in which the system is in the QSH regime is reduced, assuming the same value of $\lambda_{so} = 0.1t$. To gain a more quantitative insight we analyze the magnitude of $\mathcal{M}_{ik}$ as a function of energy E and spin-orbit coupling strength λ_{so} for both models [Figs. 2(a) and 2(b)]. In the case of the standard Kane-Mele model, the QSH regime spans the spin-orbit band gap $\Delta_{so} = 6\sqrt{3}\lambda_{so}$ [dashed lines in Fig. 2(a)]. For the modified Kane-Mele model we also find a linear dependence of the QSH energy range on λ_{so}, although scaled down by approximately a factor of 5 compared to the former case. In both cases, the direction of the edge-state electron spins is along the z axis by construction [Eq. (1)]. Another important difference between the two models is the width dependence of the results. In the case of the standard Kane-Mele model, the QSH energy range is independent of nanoribbon width. However, it decays with increasing the nanoribbon width for the modified Kane-Mele model due to the decrease of the energy gap between bulklike valence and conduction bands.

We note that the Rashba spin-orbit term has been omitted in our model. It was demonstrated by Kane and Mele that while the Rashba term violates the conservation of S_z, the QHS phase is present for the values of the Rashba parameter $\lambda_R < 2\sqrt{3}\lambda_{so}$.[24] Similarly, for the modified edge-only

Kane-Mele model, our calculations show that the QSH state persists for $\lambda_R \lesssim \lambda_{so}$.

We would now like to discuss the possible competing role of electron-electron interactions in graphene systems with locally induced spin-orbit interactions. For the purpose of our discussion we introduce into our Hamiltonian the Hubbard term of the form

$$\mathcal{H}' = U \sum_i n_{i\uparrow} n_{i\downarrow}, \tag{3}$$

where $n_{i\sigma} = c^\dagger_{i\sigma} c_{i\sigma}$ is the spin-resolved electron density on site i and $U > 0$ defines the magnitude of the on-site Coulomb repulsion. For practical reasons, we evaluate this term using the mean-field approximation

$$\mathcal{H}'_{mf} = U \sum_i (n_{i\uparrow}\langle n_{i\downarrow}\rangle + n_{i\downarrow}\langle n_{i\uparrow}\rangle - \langle n_{i\downarrow}\rangle\langle n_{i\uparrow}\rangle). \tag{4}$$

In the absence of spin-orbit coupling the introduction of electron-electron interactions results in a magnetically ordered state characterized by ferromagnetic correlations along the edges and antiferromagnetic correlations across the nanoribbon.[25,26] The state is gapped, as shown in the schematically depicted band structure [AF ($\lambda_{so} = 0$) in Fig. 2(c)] and breaks time-reversal symmetry. Spin-orbit interactions break the valley symmetry [AF in Fig. 2(c)] and result in a band gap closing above some critical spin-orbit interaction strength λ^{c1}_{so}.[27] The new phase is a valley half metal [HM in Fig. 2(c)]. A further increase of the spin-orbit interaction strength above λ^{c2}_{so} suppresses the magnetic ordering, thus reestablishing the QHS state and time-reversal symmetry [QSH in Fig. 2(c)]. For the two discussed models we calculate the critical values of λ_{so} assuming $U/t = 1$, consistent with the results of first-principles calculations and several experimental investigations.[28] In the case of a full Kane-Mele model treatment [Fig. 1(a)] we find $\lambda^{c1}_{so} = 0.026t$ and $\lambda^{c2}_{so} = 0.048t$. Restricting the range of spin-orbit interactions to edge atoms only [Fig. 1(c)] extends the domain of existence of the AF phase to $\lambda^{c1}_{so} = 0.106t$ while the QSH phase emerges at $\lambda^{c2}_{so} = 0.118t$ ($\approx$0.3 eV). It is worth noting that the latter value is well below the atomic spin-orbit splittings in many heavy elements [e.g., 0.49 eV in Te and 1.25 eV in Bi (Ref. 29)], thus confirming the possibility of realizing the QSH phase in edge-functionalized narrow graphene nanoribbons, even in the presence of competing electron-electron interactions. Moreover, the interplay between the effects of spin-orbit and electron-electron interactions can be controlled to some degree by changing the crystallographic orientation of the edges.[30,31]

In order to provide a proof of concept of the presented model, we performed a detailed first-principles investigation of realistic models of graphene nanoribbons with edges terminated by functional groups containing heavy elements. Our first-principles calculations were performed within the density functional theory framework employing the local density approximation (LDA) as implemented in the QUANTUM ESPRESSO package.[32] Spin-orbit effects were accounted for using fully relativistic pseudopotentials acting on valence electron wave functions represented in the two-component spinor form.[33] A plane-wave cutoff of 30 Ry was used for the wave functions. Atomic positions were fully relaxed. The convergence of the results against the plane-wave cutoff has been checked. The validity of the pseudopotentials was confirmed by comparison with the results of full-potential calculations.[34] Below, we focus on two representative examples involving tellurium (Te), a heavy element with large atomic spin-orbit splitting[29] and chemical properties very similar to those of isoelectronic sulfur for which synthetic organic chemistry is well established. The atomic configurations of the proposed model systems are motivated by the recent advances in producing atomically precise graphene nanoribbons, as discussed below. The first configuration represents a 1-nm-wide armchair graphene nanoribbon with edge termination composed of very stable tellurophene fragments. Such narrow armchair nanoribbons can be produced with atomic precision using the recently developed chemical self-assembly route.[35] Fairly complex nanostructures based on thiophene units (the sulfur analog of tellurophene) can be synthesized using standard organic chemistry methods (for examples, see Ref. 36). The second configuration is a zigzag graphene nanoribbon with a larger Te coverage density at the edges. The sulfur analogs of such nanostructures have been produced recently by fusing sulfur-rich precursor molecules inside a carbon nanotube matrix through heating or electron beam irradiation.[37,38] In order to account for the experimentally observed out-of-plane deformation resulting from the steric repulsion of Te atoms at the edge, we consider a supercell model composed of six unit cells.

Figure 3(c) shows the band structure of a Te-terminated armchair nanoribbon [Fig. 3(a)]. The parabolic valence and conduction bands with extrema at $k = 0$ and the presence of a direct band gap of 0.42 eV are typical for π-symmetry states subjected to quantum confinement in armchair graphene nanoribbons.[20] However, we note the presence of an additional band at $\approx$0.5 eV above the conduction band maximum which displays a clear Rashba-type splitting ($\alpha_R = 0.014$ eV Å) and a large magnitude of $\mathcal{M}_{ik}$. Analysis of the spatial distribution of the Rashba-split states [Fig. 3(d) for the momentum and the energy indicated by label A in Fig. 3(c)] shows that they are formed by the hybridization of edge C and Te orbitals. These electronic states are spin degenerate but localized at the opposite edges (that is, spin filtered); the spin is oriented along the y direction. Strictly speaking, such a system is not in the QSH regime, but this example proves that the edge functionalization of graphene nanoribbons can result in strong spin-orbit driven effects, in particular, the emergence of spin-filtered edge states.

We will now discuss the second model characterized by a significantly larger coverage density of Te atoms on the edges. In this case, hybridization of graphene π states with Te orbitals strongly modifies the band-structure features that are typical for zigzag graphene nanoribbons passivated by "neutral" functional groups such as hydrogen atoms. However, we note the dominance of low-dispersion bands close to the Fermi level ($E = 0$) remnant of the edge-state flat band in H-terminated graphene nanoribbons. As in the previous model, the ground state configuration of the Te-terminated zigzag nanoribbons shows no magnetic ordering, hence time-reversal symmetry is preserved. The spatial orientation of the spin is also along the y direction. Importantly, the electronic bands at low energies form a number of crossings at the Kramers degeneracy points $k = 0$ and $k = \pi/a$ characterized by large magnitudes of

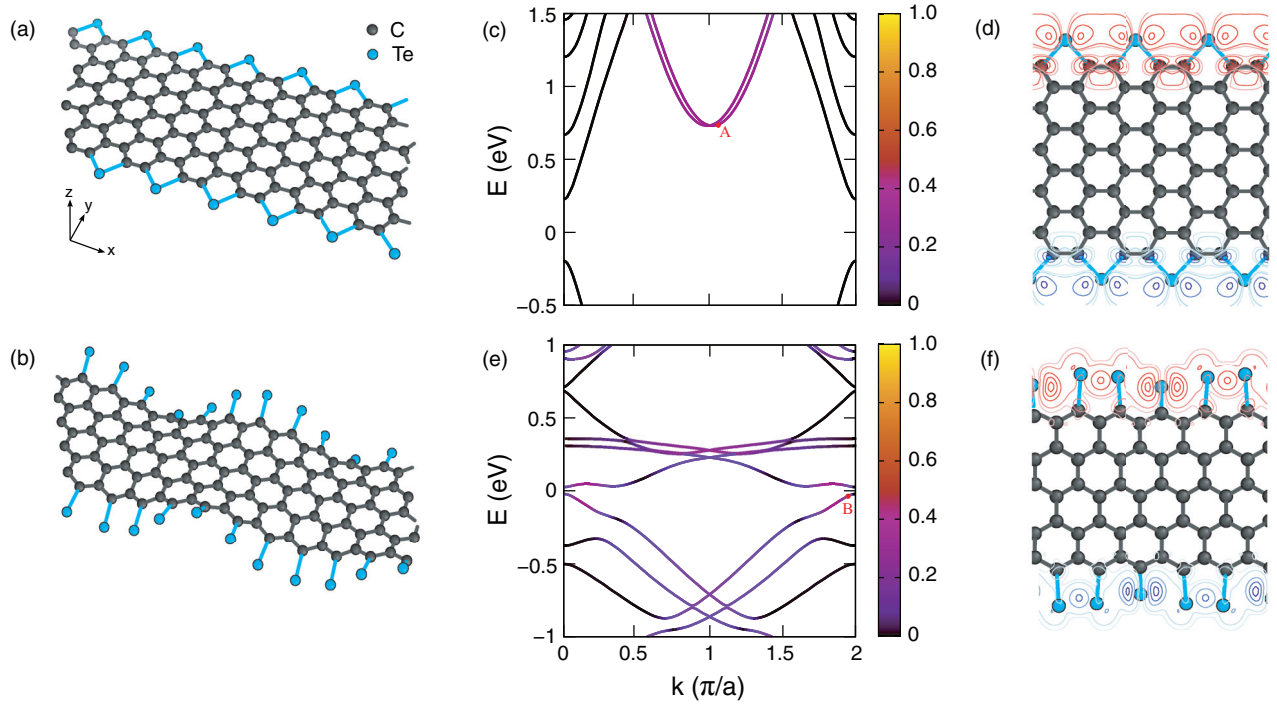

FIG. 3. (Color online) Relaxed atomic structures of Te-terminated (a) armchair and (b) zigzag graphene nanoribbons. (c) Electronic band structure of the Te-terminated armchair graphene nanoribbon with color coding indicating the magnitude of $\mathcal{M}_{ik}$. The energy is given relative to the Fermi level. (d) Contour plot of the spatial distribution of spin-filtered edge states labeled A in the band structure in (c). The spin-filtered states with opposite spin directions are distinguished by color. (e) Band structure and (f) spatial distribution of spin-filtered edge states (labeled B) in the Te-terminated zigzag graphene nanoribbon.

$\mathcal{M}_{ik}$. One such crossing, even though characterized by a band gap opening of 47 meV, is situated at the Fermi level of the charge-neutral graphene nanoribbon [Fig. 3(e)]. We ascribe the gap opening to the hybridization between the edge states localized at the opposite edge of the nanoribbon analogous to the band gaps observed in thin films of bulk topological insulators.[39–41] Importantly, there are no other bands present in the energy range $-0.32\ \text{eV} < E < 0.26\ \text{eV}$. The corresponding states are spin filtered and the system is in the QSH regime in this energy range. The relevant electronic states are mostly Te derived, as shown in Fig. 3(f).

To summarize, we proposed a method for engineering spin-orbit interactions in graphene by means of the covalent chemical functionalization of the edges. First-principles calculations performed on realistic models of tellurium-terminated graphene nanoribbons demonstrate the efficiency of our approach and the possibility of realizing the quantum spin Hall state spanning broad energy ranges. Our work thus opens up perspectives for controlling spin-orbit interactions as well as the practical realization of topological electronic phases in graphene nanostructures by means of bottom-up chemical routes.

We would like to thank M. Franz and Z. Zhu for discussions. This work was supported by the Swiss National Science Foundation (Grant No. PP00P2_133552) and by the Swiss National Supercomputing Centre (CSCS) under Projects No. s336 and No. s443.

[1] C. L. Kane and E. J. Mele, Phys. Rev. Lett. **95**, 226801 (2005).
[2] J. E. Moore, Nature (London) **464**, 194 (2010).
[3] M. Z. Hasan and C. L. Kane, Rev. Mod. Phys. **82**, 3045 (2010).
[4] X.-L. Qi and S.-C. Zhang, Rev. Mod. Phys. **83**, 1057 (2011).
[5] J. C. Boettger and S. B. Trickey, Phys. Rev. B **75**, 121402(R) (2007).
[6] M. Gmitra, S. Konschuh, C. Ertler, C. Ambrosch-Draxl, and J. Fabian, Phys. Rev. B **80**, 235431 (2009).
[7] S. Konschuh, M. Gmitra, and J. Fabian, Phys. Rev. B **82**, 245412 (2010).
[8] A. H. Castro Neto and F. Guinea, Phys. Rev. Lett. **103**, 026804 (2009).
[9] M. Gmitra, D. Kochan, and J. Fabian, arXiv:1303.2806.
[10] S. Abdelouahed, A. Ernst, J. Henk, I. V. Maznichenko, and I. Mertig, Phys. Rev. B **82**, 125424 (2010).
[11] C. Weeks, J. Hu, J. Alicea, M. Franz, and R. Wu, Phys. Rev. X **1**, 021001 (2011).
[12] H. Jiang, Z. Qiao, H. Liu, J. Shi, and Q. Niu, Phys. Rev. Lett. **109**, 116803 (2012).
[13] H. Zhang, C. Lazo, S. Blügel, S. Heinze, and Y. Mokrousov, Phys. Rev. Lett. **108**, 056802 (2012).
[14] K. T. Chan, J. B. Neaton, and M. L. Cohen, Phys. Rev. B **77**, 235430 (2008).

[15]O. V. Yazyev and A. Pasquarello, Phys. Rev. B **82**, 045407 (2010).
[16]V. M. Pereira, F. Guinea, J. M. B. Lopes dos Santos, N. M. R. Peres, and A. H. Castro Neto, Phys. Rev. Lett. **96**, 036801 (2006).
[17]O. V. Yazyev and L. Helm, Phys. Rev. B **75**, 125408 (2007).
[18]A. H. Castro Neto, F. Guinea, N. M. R. Peres, K. S. Novoselov, and A. K. Geim, Rev. Mod. Phys. **81**, 109 (2009).
[19]F. D. M. Haldane, Phys. Rev. Lett. **61**, 2015 (1988).
[20]K. Nakada, M. Fujita, G. Dresselhaus, and M. S. Dresselhaus, Phys. Rev. B **54**, 17954 (1996).
[21]S. Ryu and Y. Hatsugai, Phys. Rev. Lett. **89**, 077002 (2002).
[22]O. V. Yazyev, Acc. Chem. Res. (2013), doi: 10.1021/ar3001487.
[23]M. Wimmer, A. R. Akhmerov, and F. Guinea, Phys. Rev. B **82**, 045409 (2010).
[24]C. L. Kane and E. J. Mele, Phys. Rev. Lett. **95**, 146802 (2005).
[25]M. Fujita, K. Wakabayashi, K. Nakada, and K. Kusakabe, J. Phys. Soc. Jpn. **65**, 1920 (1996).
[26]Y.-W. Son, M. L. Cohen, and S. G. Louie, Nature (London) **444**, 347 (2006).
[27]D. Soriano and J. Fernández-Rossier, Phys. Rev. B **82**, 161302(R) (2010).
[28]O. V. Yazyev, Phys. Rev. Lett. **101**, 037203 (2008).
[29]K. Wittel and R. Manne, Theor. Chem. Acc. **33**, 347 (1974).
[30]O. V. Yazyev, R. B. Capaz, and S. G. Louie, Phys. Rev. B **84**, 115406 (2011).
[31]G. Autès and O. V. Yazyev, Phys. Status Solidi RRL **7**, 151 (2013).
[32]P. Giannozzi *et al.*, J. Phys.: Condens. Matter **21**, 395502 (2009).
[33]A. Dal Corso and A. Mosca Conte, Phys. Rev. B **71**, 115106 (2005).
[34]See Supplemental Material at http://link.aps.org/supplemental/10.1103/PhysRevB.87.241404 for the validation of the computational methodology.
[35]J. Cai, P. Ruffieux, R. Jaafar, M. Bieri, T. Braun, S. Blankenburg, M. Muoth, A. P. Seitsonen, M. Saleh, X. Feng, K. Müllen, and R. Fasel, Nature (London) **466**, 470 (2010).
[36]K. Y. Chernichenko, V. V. Sumerin, R. V. Shpanchenko, E. S. Balenkova, and V. G. Nenajdenko, Angew. Chem. Int. Ed. **45**, 7367 (2006).
[37]A. Chuvilin, E. Bichoutskaia, M. C. Gimenez-Lopez, T. W. Chamberlain, G. A. Rance, N. Kuganathan, J. Biskupek, U. Kaiser, and A. N. Khlobystov, Nat. Mater. **10**, 687 (2011).
[38]T. W. Chamberlain, J. Biskupek, G. A. Rance, A. Chuvilin, T. J. Alexander, E. Bichoutskaia, U. Kaiser, and A. N. Khlobystov, ACS Nano **6**, 3943 (2012).
[39]C.-X. Liu, H. J. Zhang, B. Yan, X.-L. Qi, T. Frauenheim, X. Dai, Z. Fang, and S.-C. Zhang, Phys. Rev. B **81**, 041307 (2010).
[40]O. V. Yazyev, J. E. Moore, and S. G. Louie, Phys. Rev. Lett. **105**, 266806 (2010).
[41]Y. Zhang, K. He, C.-Z. Chang, C.-L. Song, L.-L. Wang, X. Chen, J.-F. Jia, Z. Fang, X. Dai, W.-Y. Shan, S.-Q. Shen, Q. Niu, X.-L. Qi, S.-C. Zhang, X.-C. Ma, and Q.-K. Xue, Nat. Phys. **6**, 584 (2010).